THE PENNSYLVANIA STATE UNIVERSITY
SCHREYER HONORS COLLEGE

DEPARTMENT OF AEROSPACE ENGINEERING

A CONTROL ALLOCATION METHOD FOR A HELICOPTER WITH ON-BLADE CONTROL

ANDREW DAVID WILSON

Spring 2010

A thesis
submitted in partial fulfillment
of the requirements
for a baccalaureate degree
in Mechanical Engineering
with honors in Aerospace Engineering

Reviewed and approved* by the following:

Joseph F. Horn
Associate Professor of Aerospace Engineering
Thesis Supervisor

Robert G. Melton
Professor of Aerospace Engineering
Honors Adviser

* Signatures are on file in the Schreyer Honors College.

Abstract

Helicopter flight during shipboard operations or in turbulent wind conditions can result in very high pilot workload due to the unsteady air flow. Improvements in control methods or expanded control authority of the aircraft could allow the flight envelope to be expanded while decreasing the amount of compensation the pilot must put into the system to maintain stability. This thesis presents the results of a control allocation method with shared control between the traditional swashplate control surface and on-blade trailing edge flaps. Prior research has examined the use of trailing edge flaps solely for wind gust rejection; however, the present research will look at the feasibility of using the flaps for primary flight control as well.

The control architecture is based on a model-following controller which uses model inversion to derive ideal inputs from pilot stick inputs to yield more desirable response and handling from the helicopter. These ideal commands are passed through high and low pass filters to split the control signal based on frequency. The lower frequency control is passed to the swashplate while higher frequency control is passed to the trailing edge flaps. This could enable the helicopter to maintain more desirable handling qualities, even with degradation in swashplate

rate actuation. Simulations of the system are performed with both a linear model using Simulink and a full flight simulation using the GENHEL flight simulation code.

Results from a linear Simulink model demonstrate the operation of the frequency split allocation controller with degradation in swashplate rate actuation by using trailing edge flaps to handle high frequency control response. However, full flight simulation produces problems with saturation of the trailing edge flap actuators, even under normal flight conditions. With too much control being allocated to the flaps, the travel limits are quickly exceeded with the high frequency commands. To alleviate the issue, lower gains are implemented as well as reduced allocation to the flap actuators. While this allows the system to perform with normal handling quality, there is little qualitative difference in handling between the pure swashplate system and the shared control, even under degradation of the swashplate actuators. The results suggest that while primary control can be allocated to the flaps, there are serious limitations in the current travel limits of the flaps and the ability to handle the control input without reaching saturation limits. Under controlled circumstances, the benefit of the added control may be realized; however, in normal flight simulation, minimal qualitative difference is recorded.

Table of Contents

List of Figures

List of Tables

List of Symbols

p	Vehicle roll rate
q	Vehicle pitch rate
r	Vehicle yaw rate
ϕ	Vehicle roll attitude
θ	Vehicle pitch attitude
ψ	Vehicle heading
δ_{lat}	Lateral swashplate deflection
δ_{long}	Longitudinal swashplate deflection
δ_{ped}	Pedal deflection
δ_{1c}	Lateral TEF deflection
δ_{1s}	Longitudinal TEF deflection
ω_n	Actuator natural frequency
ζ	Actuator damping ratio
τ	Frequency splitting time constant
e	Angular tracking error
ν	Pseudo-commands
K_P, K_D, K_I	PID controller gains
A, B	State space representation of aircraft model

Acknowledgments

I am incredibly thankful to everyone who has helped me complete this project. This thesis would absolutely not have been possible without the supervision of Dr. Joe Horn, my thesis advisor. I am grateful for all of the time and effort he has spent teaching me about helicopter control and simulation and assisting me with the analysis and testing of the flight control laws. I would like to acknowledge Dr. Ed Smith, Director of the Penn State Vertical Lift Research Center of Excellence, as well for his time and contributions to the project. Additionally, I want to thank Eric O'Neill for his knowledge and assistance with the GENHEL simulation code and help during the flight simulator tests.

Lastly, thanks to my family and friends who have supported me throughout my college career. I would certainly not have made it to this point without everything you have done for me.

Chapter 1

Introduction

1.1 Background and Motivation

1.1.1 Challenges of Wind Gust Disturbances

In the area of helicopter flight control, operation of the helicopter in high wind, particularly in shipboard operations, is still a challenging maneuver which requires significant pilot workload. This high workload is a major safety issue that must be considered during shipboard operations or in highly turbulent wind conditions. During takeoff and landing operations, the extra workload due to wind gusts contributes to the already elevated pilot workload. The issue of safety has led to strict flight operation conditions, including a wind flight envelope for shipboard operations. Improvements in helicopter gust rejection would result in a decreased pilot workload, potentially reducing limitations on flight due to high turbulence and providing increased control authority to the pilot.

Most current rotorcraft flight control systems use limited authority stability augmentation systems (SAS) to provide additional stability to the helicopter. While these systems are effective, the flight envelopes are still limited. During shipboard operations, pilots must take into account this limited envelope. Figure 1.1 shows an example of a wind over deck envelope which is a diagram for pilots indicating allowable areas to fly depending on wind speed and direction. These flight envelopes are determined by extensive simulation and flight tests. A limitation of the helicopter hardware includes the rate and travel limits of the swashplate actuations which add delay and nonlinearity into the feedback system. With new

ideas such as using on-blade flaps, or elevons, that function as additional control surfaces, the control authority of the helicopter could be increased. This could allow the flight envelope for conditions such as shipboard operations to be expanded or at least improve function under degraded conditions on the swashplate mechanism.

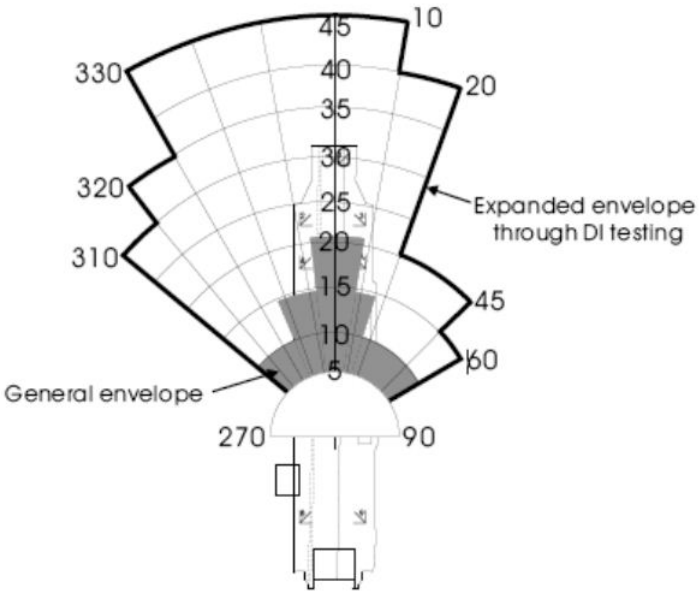

Figure 1.1. Example of a ship wind over deck (WOD) flight envelope [1].

1.1.2 Current Helicopter Control

Most helicopters in production today rely solely on traditional swashplate control. The swashplate mechanism converts control inputs from the fixed frame of the helicopter fuselage to the rotating frame of the helicopter blade. Through a series of hydraulics and pitch links, the pitch of the rotor blades is adjusted, changing the lift of the blades and moment on the helicopter fuselage. These pitch links can create periodic inputs for each revolution of the rotor blades (1/rev). This enables lateral and longitudinal control of the helicopter which results from changes in the roll and pitch attitude of the helicopter body. A photo of the swashplate assembly on a UH-60 helicopter can be seen in Figure 1.2. Using the conventional swashplate system, flight controls have been developed to minimize the pilot's workload during

normal flight operations, and requirements have been implemented such as the ADS-33 specification which mandates levels of required stability and control for military rotorcraft [2]. Levels of handling quality range from Level 1, which is desirable handling, to Level 3, which is undesirable [3].

Additionally, pilots are trained for situations where there is a degradation of control function in the swashplate controls. In redundant hydraulic systems, the loss of one actuator would result in a 50% decrease in power. This reduces the maximum velocity and acceleration of the control surface. With this loss, the controls can degrade into Level 3 handling. With proper training, pilots can maintain control of the aircraft but with a much higher workload [4].

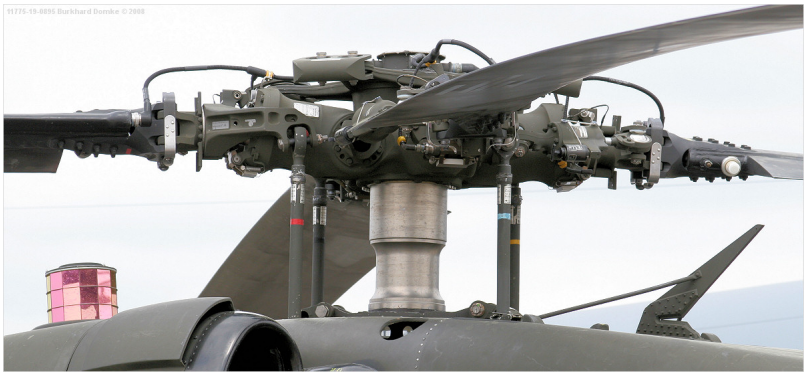

Figure 1.2. UH-60 swashplate assembly [5].

1.1.3 Control with Trailing Edge Flaps

Another idea that has been proposed for rotorcraft control uses on-blade trailing edge flaps. Mechanisms such as servo flaps have already been successfully demonstrated on helicopters such as the Kaman helicopters. New smart materials and piezoelectrics are being developed which could be incorporated directly into the blade to actuate a flap as a different control surface for the helicopter. The flaps have undergone several full scale wind tunnel tests, including tests for vibration control such as the test for the SMART rotor seen in Figure 1.3. These trailing edge flaps were originally studied for use in vibration control using methods similar to individual blade control (IBC) and higher harmonic control (HHC).

There has been significant research into the use of trailing edge flaps which will be detailed in the literature survey. Applications have expanded from vibration

and noise control, to primary flight control, to disturbance rejection methods. The trailing edge flaps can be used as an additional control surface, creating a moment on the rotor hub with changes in the flap deflection. In this way, the flap can be used in a similar control method as the swashplate control surface.

Figure 1.3. Trailing edge flap on SMART rotor [6].

1.2 Literature Survey

1.2.1 Helicopter and Gust Modeling

A number of studies have been performed on the topic of wind gust alleviation for pilot control [7, 8, 9]. A paper was presented by Dr. Joe Horn and Derek Bridges on a controller designed for gust rejection during shipboard operations. This study uses a basic model following control scheme with an additional airwake rate compensator to reject ship airwake disturbances. This control method seen in Figure 1.4 resulted in qualitative handling improvements in simulation.

An advantage of the model following control architecture is that it maintains similar response to pilot commands since it calculates the ideal response of the aircraft based on roll, pitch, and yaw natural frequency and damping for Level 1 handling. Assuming there is no disturbance to the aircraft, feedback is only used to correct model inversion error. Pseudo-commands based on the angular tracking

error provide an ideal pilot command based on the helicopter dynamics.

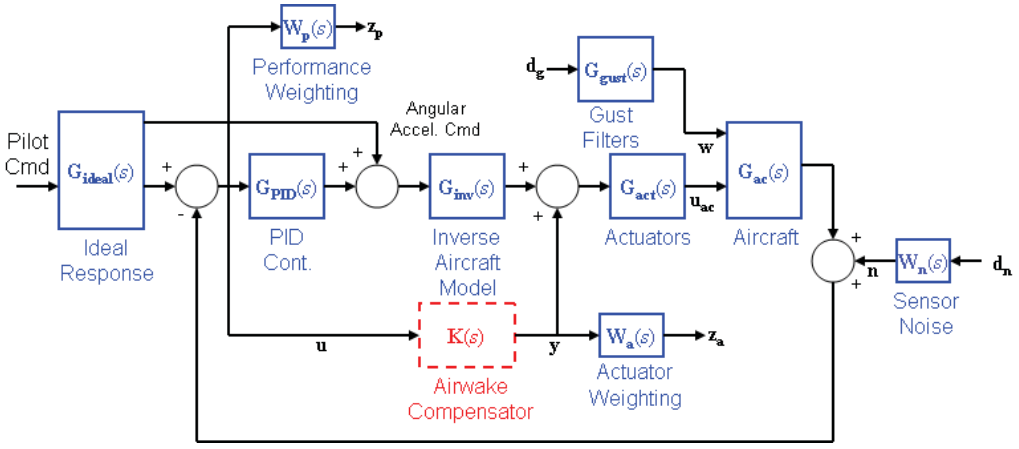

Figure 1.4. Model following controller with airwake compensation [9].

The model, when optimized for the UH-60A helicopter, showed that the airwake compensator used in the model following control architecture significantly reduced the rate response of the aircraft in simulated high wind conditions. The simulation was conducted using an aircraft model in a turbulent airwake on an LHA ship under 30 knot/30 degree wind over deck conditions. The model following controller will also serve as the basis controller for the control allocation research in this thesis.

1.2.2 Trailing Edge Flap Research

There has been significant and ongoing research with regards to using trailing edge flaps as a control surface for helicopters. Numerous studies have been performed on the aerodynamics of these flaps. In Shen and Chopra's study, the properties of the flaps were studied for vibration control [10]. The study showed that the flaps could be effective in reducing 5/rev vibratory loads on the hub of the helicopter. Another study by Milgram, et al, found that using 3/rev and 4/rev flap inputs could also lead to a high reduction in vertical hub vibratory loads [11].

The trailing edge flap idea has also been studied as a backup system for swash-plate control. Research was conducted on the feasibility of using a trailing edge flap to control a blade with a severed pitch link, which eliminates the swashplate control functionality for the individual blade. The study found that with high flap deflection, the flap could be used to make the blade respond similarly to one

driven by the swashplate in flapping motion [12]. This presents another scenario for the use of trailing edge flaps as emergency control surfaces. Further research has begun to look into the use of the flaps as primary control surfaces instead of for purely vibrational or emergency control.

1.2.2.1 Flaps for Primary Control

After initial research into the trailing edge flap model, studies have been performed to determine the feasibility of using these flaps as a primary control surface. Jinwei Shen at the University of Maryland performed an analysis on the aeroelasticity of trailing edge flaps and expanding the use from vibration control to primary flight control. The study provided an analytical model for the analysis of on-blade trailing edge flaps [13]. In the dissertation, parameters for the trailing edge flaps were developed, including the size of the flaps, the pitch link stiffness, and other parameters. Further studies have attempted to find optimal parameters for the trailing edge flaps.

Some data suggests eliminating the swashplate system in favor of exclusive control with on-blade trailing edge flaps. Several studies have been performed to evaluate the feasibility of using swashplateless control systems for helicopters [14, 15]. The advantage of swashplateless systems is the ability to reduce the mechanical complexity of the hydraulic actuators and swashplate mechanism. This could result in lower hub drag and improvements in performance. Although these studies have shown promise in the capabilities of swashplateless systems to perform maneuvers requiring great control authority, the swashplate system still provides increased control authority, including sufficient collective control to trim the helicopter.

A thesis by Christopher Duling at Penn State University examines using variable RPM to decrease the required flap input and power requirements when using the trailing edge flaps for primary control [16]. Duling studied the feasibility of trimming the swashplateless helicopter under various gross weights using the variable RPM. The study showed that increased RPM could improve the trim requirement for most situations. The overall power requirement increased, however, for the swashplateless system over the conventional swashplate model.

1.2.2.2 Flaps for Gust Rejection

A great deal of research is now being performed on trailing edge flaps for helicopter control. On-blade flaps allow for individual blade control and have been studied as a means of vibration reduction, noise control, and primary helicopter control. A recent thesis by Ms. Pamela Montanye examined the use of trailing edge flaps as a device for gust alleviation in addition to primary control by the helicopter swashplate [17]. A controller based on H_2 control theory is implemented along with the basic model following controller.

The control law is modeled after the control architecture by Horn and Bridges[9] but uses trailing edge flaps as the gust actuators instead of swashplate actuators. The H_2 controller provides the disturbance rejection, taking tracking error and producing trailing edge flap commands to the aircraft. The swashplate motion is produced by traditional PID control based on the same tracking error. This study finds that trailing edge flap control can help alleviate the vehicle gust response significantly in the roll axis and result in modest improvement in the pitch axis.

1.3 Current Research Focus

As stated in the literature survey, there has been a depth of research performed on the feasibility of trailing edge flap use for primary control. There have also been studies on the use of trailing edge flaps strictly for disturbance rejection using the model following control architecture. The scope of this research is to develop a method to use the trailing edge flaps as a shared primary control surface in addition to the traditional swashplate control. In this way, the trailing edge flaps should act as an extension of the swashplate control, with both surfaces performing wind gust disturbance rejection.

The emphasis of the research will concern the use of trailing edge flaps as faster actuators, possibly extending the frequency range which can be achieved by traditional swashplate control. The control allocation architecture will compare the handling of the aircraft under swashplate control and shared control. The research will also examine the use of the trailing edge flaps under degraded swashplate conditions in the form of rate limits on the swashplate actuators.

Chapter 2

Control Development

The helicopter flight control system will include two separate control surfaces - the swashplate system and the trailing edge flap system. Previous research has yielded models for both control surfaces which will be used for control design and evaluation. For this thesis, both systems will be used for primary flight control; however, the systems will operate in different frequency ranges. The swashplate system will control lower frequency control inputs while the on-blade trailing edge flaps will control the higher frequency inputs.

Using this control allocation method will allow the swashplate actuators to work in a lower frequency state for large, low frequency maneuvers as well as provide collective control to trim the aircraft. In the higher frequency range, the trailing edge flaps can accommodate smaller amplitude but higher frequency control for maneuvers, including disturbance rejection. In this capacity, the trailing edge flap system is an extension of the swashplate control surface.

The primary control system uses a model following control architecture which is detailed by prior research by Horn, et al [9]. The controller feeds forward pilot input commands and creates pseudo-commands that are allocated to the swashplate and trailing edge flaps.

2.1 Aircraft and Simulation Models

The aircraft model used for control development is a linearized model derived from the nonlinear GENHEL (General Helicopter) flight dynamic simulation code[18] which includes dynamics for the trailing edge flap models. This simulation code

was originally developed by Sikorsky Aircraft, with extensive models including the aerodynamics of the main rotor, fuselage, empennage, and tail rotor. Parameters used for the GENHEL simulation code and helicopter model can be found in Appendix A.

In order to use linear control methods, linear models are derived from the full GENHEL nonlinear model. The model has been linearized in hover for the purpose of the control development in this thesis. There are 28 states in the linear model which include vehicle, rotor, and engine dynamics. For the model inversion required by the model following controller, the linear model is reduced to 3 states, which are the vehicle angular rates. In this study, the model following controller is tested using the linear aircraft model in the Simulink environment. After analyzing the controller in the linear environment, a flight simulation is completed using the GENHEL environment to get final results and conclusions for the study.

The controller is also tested in the presence of a simulated ship airwake model developed by Lee, et al [19]. The gust model is based on a UH-60A helicopter operating from a landing helicopter assault (LHA) class ship. CFD simulations were performed to model the airwake and then interface the solutions with the GENHEL simulation code. The case used in this study is a 30 knot/30 degree wind over deck condition. The gust simulation also applies a stochastic airwake model for efficient simulation also developed by Lee [7]. The model extracts a six dimensional gust vector from CFD airwake models which are then driven by white noise. This enables testing of the controller in both the Simulink and GENHEL environments.

2.2 Model Following Control

The model following control method is based on angular rate tracking error. The initial pilot commands are passed through a command filter which outputs ideal responses based on Level 1 handling qualities in the ADS-33 specification. The current vehicle angular rates are then subtracted from the ideal rate responses. For the purpose of this research, PID control is used as the sole control method that creates pseudo-commands which are fed to the actuators and aircraft. The diagram of the model following control architecture with disturbance inputs can be seen in Figure 2.1.

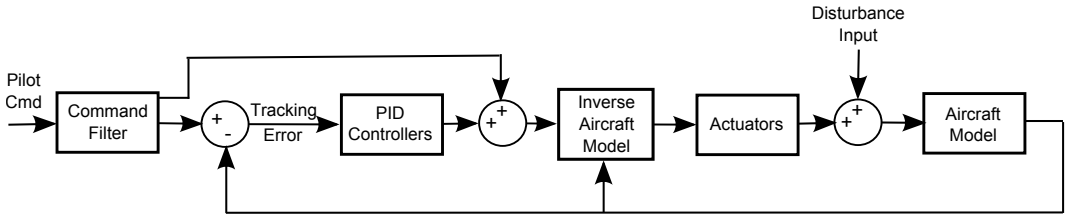

Figure 2.1. Simple model following control architecture.

2.2.1 Command Filter Model

In the model following control architecture, the pilot stick inputs are first passed through a command filter to generate the ideal response rates for roll and pitch and yaw. This ideal response model is based on ADS-33 requirements for attitude command/attitude hold (ACAH) response in the roll and pitch axes. Details on the command filter are given in studies by Horn and Monetayne. The roll and pitch axes use second order response models while the yaw axis uses a first order response model.

$$\begin{bmatrix} \phi_c \\ \theta_c \\ r_c \end{bmatrix} = \begin{bmatrix} \frac{\omega_n^2}{s^2+2\zeta\omega_n s+\omega_n^2} & 0 & 0 \\ 0 & \frac{\omega_n^2}{s^2+2\zeta\omega_n s+\omega_n^2} & 0 \\ 0 & 0 & \frac{1}{\tau s+1} \end{bmatrix} \begin{bmatrix} \phi_{cmd} \\ \theta_{cmd} \\ r_{cmd} \end{bmatrix} \tag{2.1}$$

and

$$\begin{bmatrix} \dot{\phi}_c \\ \dot{\theta}_c \\ \dot{r}_c \end{bmatrix} = \frac{d}{dt} \begin{bmatrix} \phi_c \\ \theta_c \\ r_c \end{bmatrix} \tag{2.2}$$

and

$$\begin{bmatrix} \ddot{\phi}_c \\ \ddot{\theta}_c \end{bmatrix} = \frac{d^2}{dt^2} \begin{bmatrix} \phi_c \\ \theta_c \end{bmatrix} \tag{2.3}$$

where ϕ_c and θ_c are the ideal roll and pitch Euler angles and r_c is the ideal yaw rate. ϕ_{cmd}, θ_{cmd}, and r_{cmd} are the pilot stick inputs converted to Euler angles. For

this study, the parameters used for the ideal response model are $\omega_n = 2.5$ and $\zeta = 0.8$ for the roll and pitch axes and a time contant, τ, of 0.4 in the yaw axis.

2.2.2 Error Dynamics & PID Control

After the ideal response is generated, the current body angular rates are subtracted from the ideal rates. This rate tracking error is then fed into a PID controller to stabilize the response. Previous studies have used PD control to provide similar response to the ideal response model. For this thesis, an integrator is added to the control scheme to provide better attitude response over longer time periods.

The goal of the PID controller is to drive the tracking error to zero with satisfactory rise time and damping. To determine gains for the PID controller, the equation for error dynamics is written as,

$$\ddot{e} + K_D\dot{e} + K_P e + K_I \int e = \nu \tag{2.4}$$

where,

$$\ddot{e} + K_D\dot{e} + K_P e + \int e = \nu \tag{2.5}$$

Taking the derivative of the error dynamics equation yields,

$$\dddot{e} + K_D\ddot{e} + K_P\dot{e} + K_I e = \Delta \tag{2.6}$$

Solving for the transfer function e/Δ yields,

$$\frac{e}{\Delta}(s) = \frac{1}{s^3 + K_D s^2 + K_P s + K_I} \tag{2.7}$$

The gains for the PID controller are based on the ideal second-order response with an additional pole for the integrator term. These are determined by setting the denominator of Equation 2.7 to the second-order damping and natural frequency,

along with a real pole, p, for the integral gains. This equation is given by,

$$s^3 + K_D s^2 + K_P s + K_I = (s^2 + 2\zeta\omega_n s + \omega_n^2)(s + p) \tag{2.8}$$

After factoring and solving Equation 2.8, the gains for the pitch and roll axes are given by,

$$K_P = \omega_n^2 + 2\omega_n \zeta p \tag{2.9}$$

and

$$K_D = 2\omega_n \zeta + p \tag{2.10}$$

and

$$K_I = \omega_n^2 p \tag{2.11}$$

For this study, in the roll and pitch axes, $\omega_n = 2.5$ and $\zeta = .8$. For the yaw axis, first order PI gains are used to provide similar characteristics to the ideal response mode,

$$K_P = 2\omega_n \zeta \tag{2.12}$$

and

$$K_I = \omega_n^2 \tag{2.13}$$

The yaw axis assumes a natural frequency, $\omega_n = 1/\tau$ and $\zeta = 0.9$.

After testing results for the ideal gains, it was found that more control was needed beyond the ideal response. For the purpose of this thesis, PID gains were increased to provide better tracking error. The lateral K_P and K_D gains were experimentally increased from the ideal response values. K_P is set at 3.2 times the ideal gain in the roll axis and K_D is set at 2 times the ideal value in the roll axis. The value of K_I remains the same as calculated with the ideal response gains.

2.2.3 Reduced Model Inversion

The full model is a state space system including vehicle, rotor, and engine dynamics. From this full model, many states are removed, such as the engine dynamics and rotor dynamics, until the model is reduced to a third-order angular rate model with p, q, and r. This model is then used to generate an inverse system for the model following controller. A separate third-order model is generated for the swashplate and for the trailing edge flaps. The swashplate model includes the lateral, longitudinal, and pedal inputs, and the trailing edge flap model includes δ_{1c}, δ_{1s}, and pedal inputs.

Using the state space equations for the helicopter dynamics, the equation to calculate the pseudo-commands which are used in the model following controller is:

$$\boldsymbol{\nu} = A_{pqr} \begin{bmatrix} p \\ q \\ r \end{bmatrix} + \begin{bmatrix} B_{swash} & \vdots & B_{TEF} \end{bmatrix} \begin{bmatrix} \delta_{lat} \\ \delta_{long} \\ \delta_{ped} \\ \delta_{1c} \\ \delta 1s \\ \delta_{ped} \end{bmatrix} \tag{2.14}$$

where the pseudo-command vector, $\boldsymbol{\nu}$, is the vector of ν_p, ν_q, and ν_r which are related to the tracking error by Equation 2.4 in each axis - roll, pitch, and yaw.

Using the reduced third-order models and Equation 2.14, the trailing edge flap inverse is calculated from the reduced order inverse B matrix as follows:

$$\begin{bmatrix} \delta_{1c} \\ \delta_{1s} \\ \delta_{ped} \end{bmatrix} = B_{TEF}^{-1} \left(\begin{bmatrix} \nu_p \\ \nu_q \\ \nu_r \end{bmatrix} - A_{pqr} \begin{bmatrix} p \\ q \\ r \end{bmatrix} \right) \tag{2.15}$$

Similarly, the traditional swashplate commands are found with the reduced order

swashplate B matrix:

$$\begin{bmatrix} \delta_{lat} \\ \delta_{long} \\ \delta_{ped} \end{bmatrix} = B_{swash}^{-1} \left(\begin{bmatrix} \nu_p \\ \nu_q \\ \nu_r \end{bmatrix} - A_{pqr} \begin{bmatrix} p \\ q \\ r \end{bmatrix} \right) \tag{2.16}$$

By using the reduced order matrices, the inputs to the actuators can be quickly determined. Although the use of the third-order models introduces error from the model inversion, the error tracking with the model following control architecture will compensate for the small inversion error.

2.3 Frequency Split Control Allocation

The frequency split allocation method is used to distribute the high frequency commands to the trailing edge flaps and low frequency commands to the swashplate, resulting in the correct overall control of the helicopter. This frequency split is accomplished using a first order high and low pass filter:

$$\text{high pass:} \quad \frac{\tau s}{\tau s + 1} \tag{2.17}$$

$$\text{low pass:} \quad \frac{1}{\tau s + 1} \tag{2.18}$$

The time constant, τ, serves as the frequency splitting threshold which is used to control the amount of control given to the trailing edge flaps. From the time constant, the cutoff frequency can be calculated as:

$$f_c = \frac{1}{2\pi\tau} \tag{2.19}$$

For the shared control between the trailing edge flaps and swashplate, the low frequency spectrum of command will be sent to the swashplate inputs, δ_{lat}, δ_{long}, and the high frequency command will be sent the trailing edge flap inputs, δ_{1c}, δ_{1s}. Since the pedal command is primarily given by the tail rotor, the sum of the low pass and high pass inputs will be passed to the pedal input.

Using the trailing edge flaps for high rate commands will enable the vehicle response to still be predictable even with rate limitations on the swashplate actuators. The frequency split model following controller can be seen in Figure 2.2.

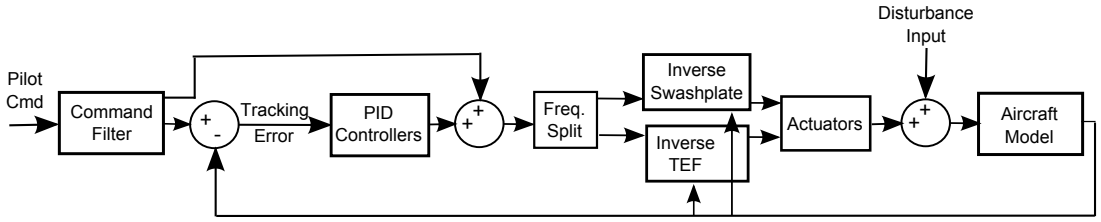

Figure 2.2. Frequency split model following control architecture.

2.4 Actuator Models

The actuators are separated into the swashplate actuators for the δ_{lat}, δ_{long}, δ_{ped} commands and the trailing edge flap actuators, δ_{1c} and δ_{1s}. The actuators are approximated by second-order transfer functions:

$$\frac{\omega_n^2}{s^2 + 2\zeta\omega_n s + \omega_n^2} \tag{2.20}$$

In the linearized helicopter model, there is an actuator response model. Rate and travel limits are applied to all commands by providing saturation limits to a feedback loop block diagram actuator model. This block diagram of the second order transfer function can be seen in Figure 2.3.

In the GENHEL simulation, rate limits can be applied to the swashplate actuators, while the trailing edge flap actuators are treated as ideal for the high frequency responses. For this study, the parameters of the actuators are $\omega_n = 40$ and $\zeta = 0.8$. For the degraded actuator environment, the natural frequency of the swashplate actuators is decreased, while the trailing edge flap is set very high to simulate ideal behavior.

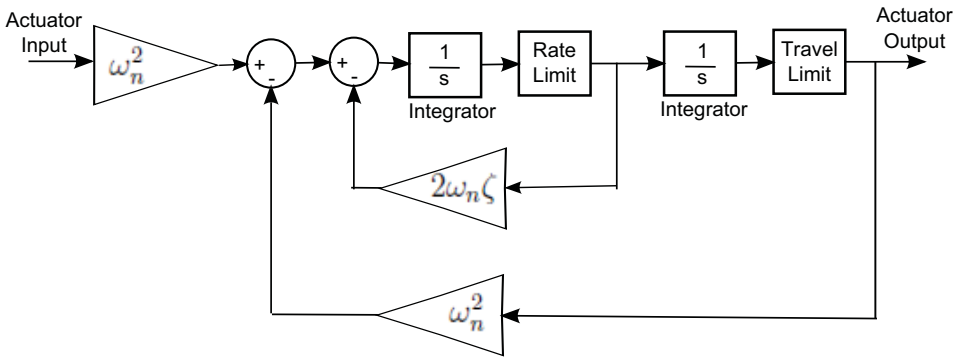

Figure 2.3. Actuator block diagram with rate & travel limits.

2.4.1 Frequency-Imposed Rate Limits

Using the frequency split control scheme inherently limits the required frequency of the swashplate controls. By using a time constant, τ, the cutoff frequency is determined where the magnitude of the rate response rolls off. Using this frequency as the cutoff, the rate of swashplate control will not exceed the specified angular frequency. Therefore, rate saturation on the swashplate actuators will have no adverse effects on the aircraft response unless it falls below the cutoff frequency, f_c. Therefore, the maximum rate that the swashplate actuators will be required to sustain for any maneuver will be directly related to $1/\tau$.

Chapter 3

Results & Discussion

Simulation of the control allocation described in Section 2.3 is performed both on the linear model aircraft system in Simulink as well as a flight simulator using the GENHEL model. The linear analysis of the model is used to show the theoretical response of the controller to controlled parameters, including the natural frequency of the actuators, rate limits of the swashplate mechanism, and the frequency allocation threshold. Additionally, the response to wind gusts is examined with different PID control schemes within the linear model. Although the results from the linear model demonstrate the potential advantages of the shared control, the results obtained with the GENHEL flight simulator tests show little qualitative benefit to sharing the primary flight control.

3.1 Analysis of Frequency Split Allocation

The analysis of the controller will primarily include qualitative flight simulation testing. Theoretical operation of the controller is shown through the linear simulation; however, the performance of the controller will be judged on the flight simulation data. Several flight simulations were performed with varying gain and swashplate degradation. In the flight simulator results, the primary pilot maneuver used to evaluate handling qualities is a doublet maneuver in the longitudinal controls. The longitudinal axis is used because of the high rate of saturation of the δ_{1s} actuator in the vehicle response.

3.1.1 PID Control Response

The PID gains were calculated in Section 2.2.2 to provide a response that would be close to the ideal response of the vehicle. Using these gains on a 4.5 degree roll maneuver, the higher gains were tested with the ship gust model in the linear Simulink simulation. Figure 3.1 shows the result of the linear simulation with respect to vehicle attitude response, and Figure 3.2 shows the vehicle rate response with respect to the Euler angles.

From this linear simulation, the results show that the higher gain in the roll axis provides better tracking in that axis. The increase in PID gain in the roll has very little effect on the pitch attitude and heading.

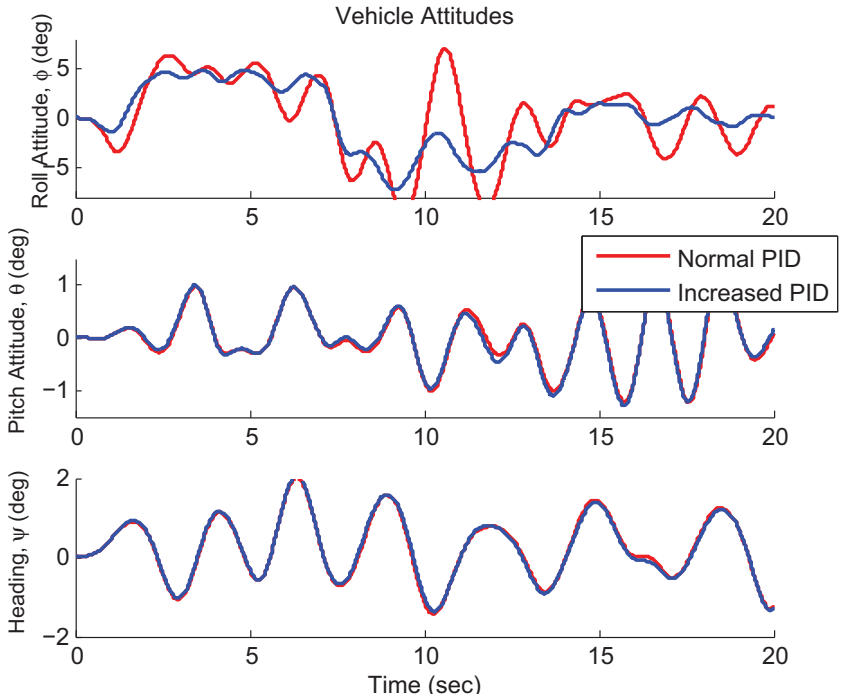

Figure 3.1. Attitude response to ship airwake model with varying PID gain.

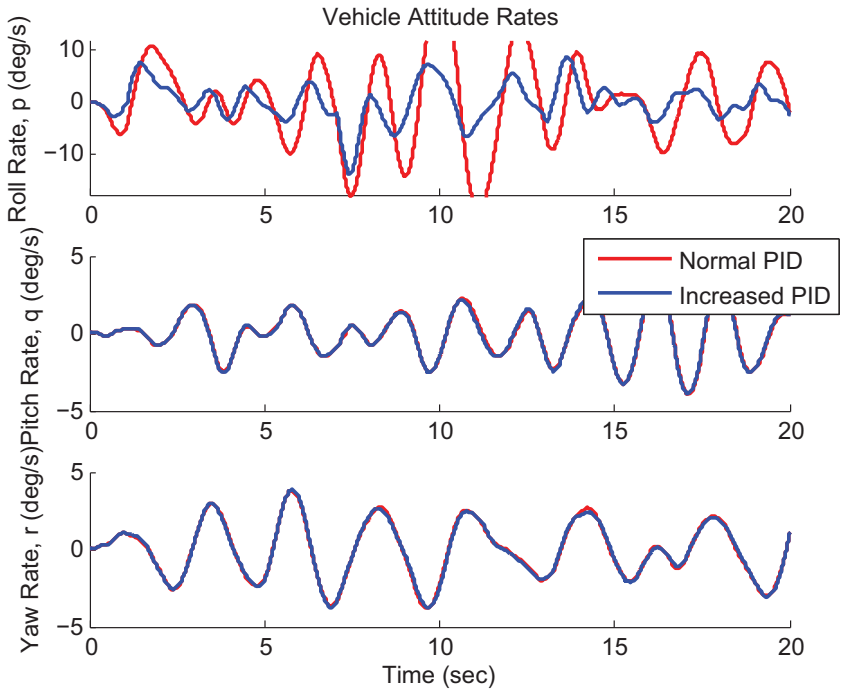

Figure 3.2. Angular rate response to ship airwake model with varying PID gain.

When tested on the flight simulator with the GENHEL model, the performance of the controller deteriorated due to larger pilot deflections. The response in the pitch axis is highly undamped due to saturation of the δ_{1s} actuators. Figure 3.3 shows the pitch attitude response of the vehicle in the GENHEL simulation and the pilot's commanded stick input.

The same pilot command was then used in the Simulink linear simulation to determine if the linear simulation would match the GENHEL results. Figure 3.4 shows the result of the comparison in the pitch attitude response. The result shows that the linear model does show the same undamped behavior due to the saturation of the trailing edge flap actuators.

Figure 3.4 shows the response of the δ_{1s} actuators. The result shows that the actuators clearly hit the defined travel limits which causes the highly undamped vehicle response. This response is highly undesirable in flight and shows the limitations of high PID gains.

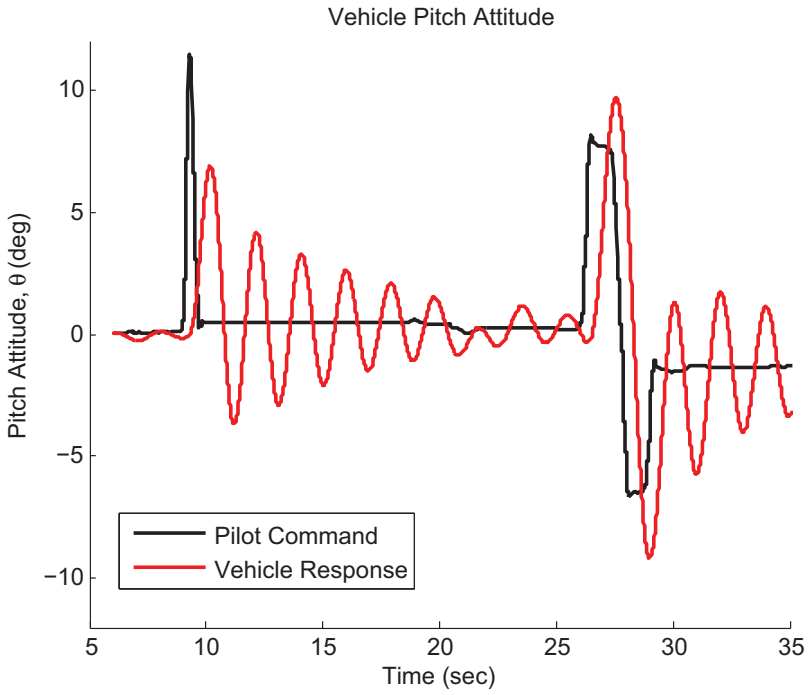

Figure 3.3. Pitch attitude response with increased pitch gain.

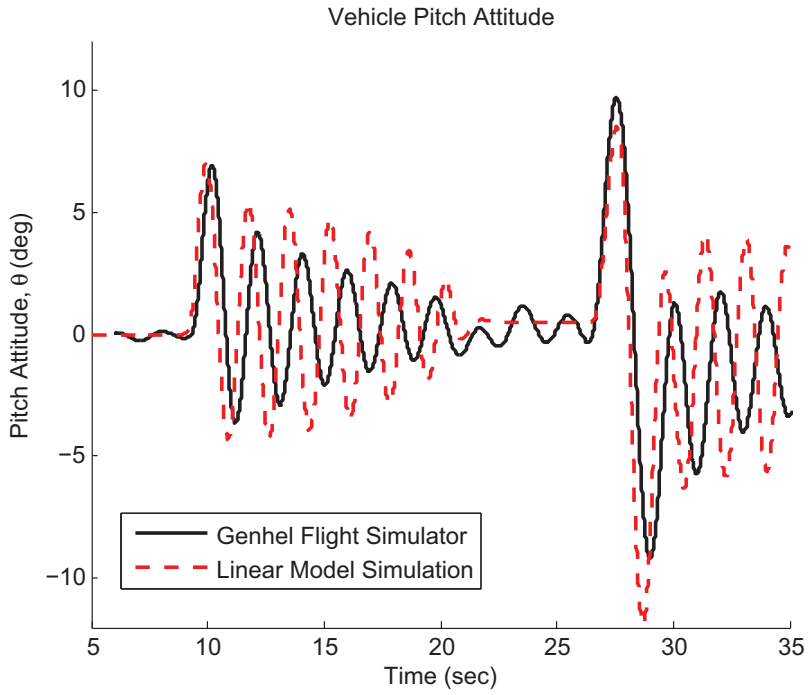

Figure 3.4. Comparison of flight simulation to linear simulation with increased pitch gain.

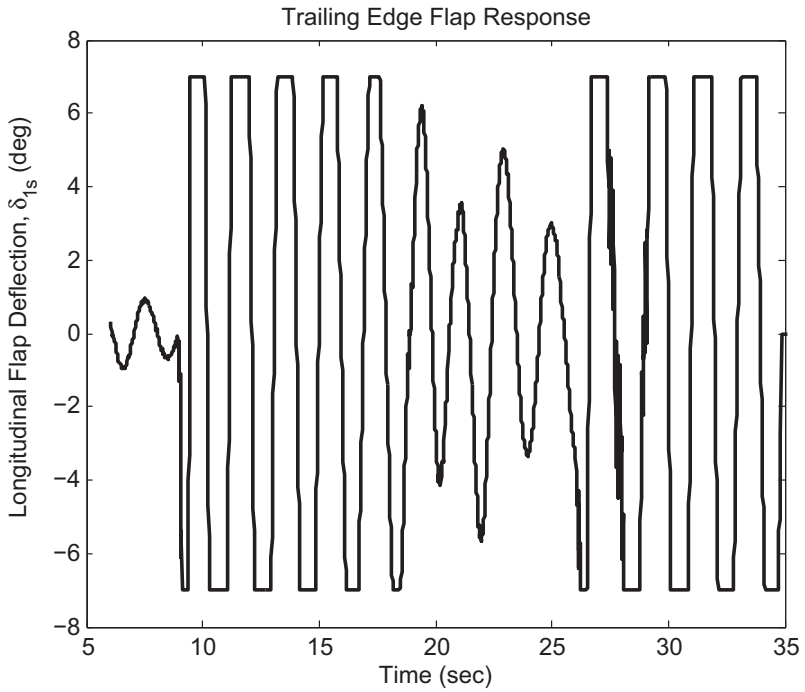

Figure 3.5. δ_{1s} flap response with ± 7 deg saturation and increased pitch gain.

Because of the saturation of the δ_{1s} actuators in normal flight, the gains are reduced to the ideal levels for the remaining flight tests. The ideal response PID control gains are calculated in Section 2.2.2. The reduced gains result in more desirable flight simulations as seen in the attitude response in Figure 3.6.

The pilot command is once again used in the linear Simulink model and compared to the GENHEL results in Figure 3.7. The result shows that the linear model compares well to the nonlinear GENHEL model using the trailing edge flap actuators.

Figure 3.8 shows the response of the δ_{1s} actuators. As seen in the result, the actuators still reach their travel limits during the test; however, it is not to a degree that significantly affects the vehicle response. Larger pilot commands or disturbances could cause more significant saturation which could lead to undesirable handling qualities.

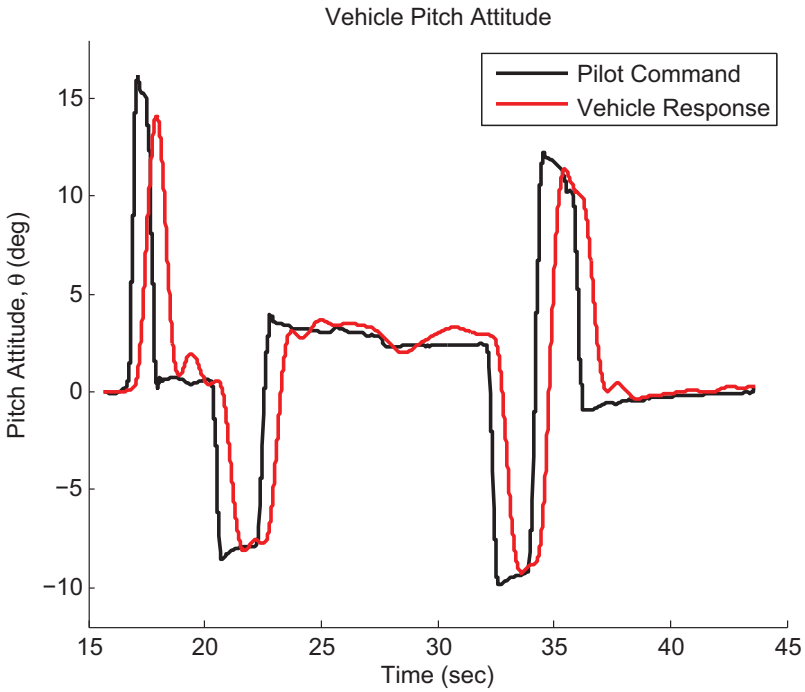

Figure 3.6. Pitch attitude response with decreased pitch gain and frequency splitting threshold.

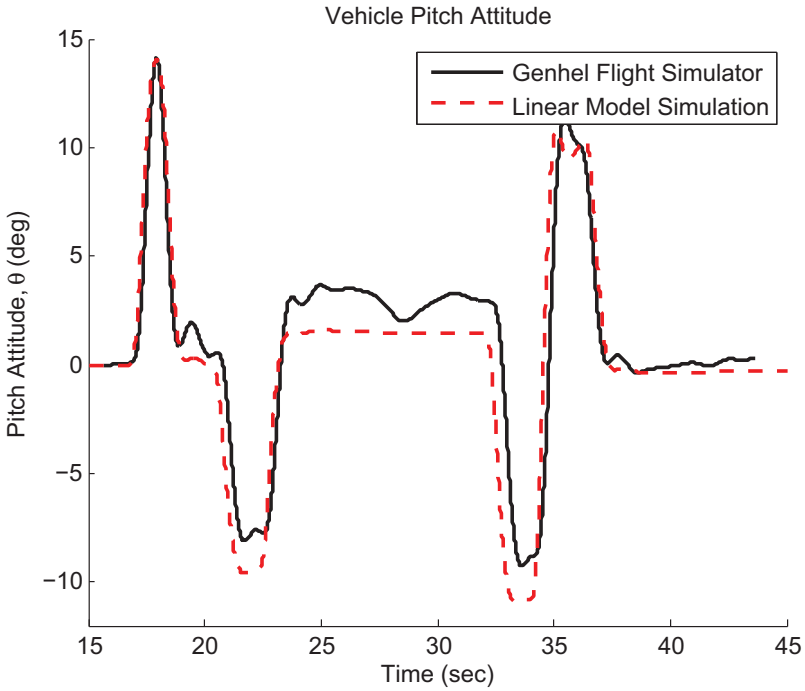

Figure 3.7. Comparison of flight simulation to linear simulation with decreased pitch gain.

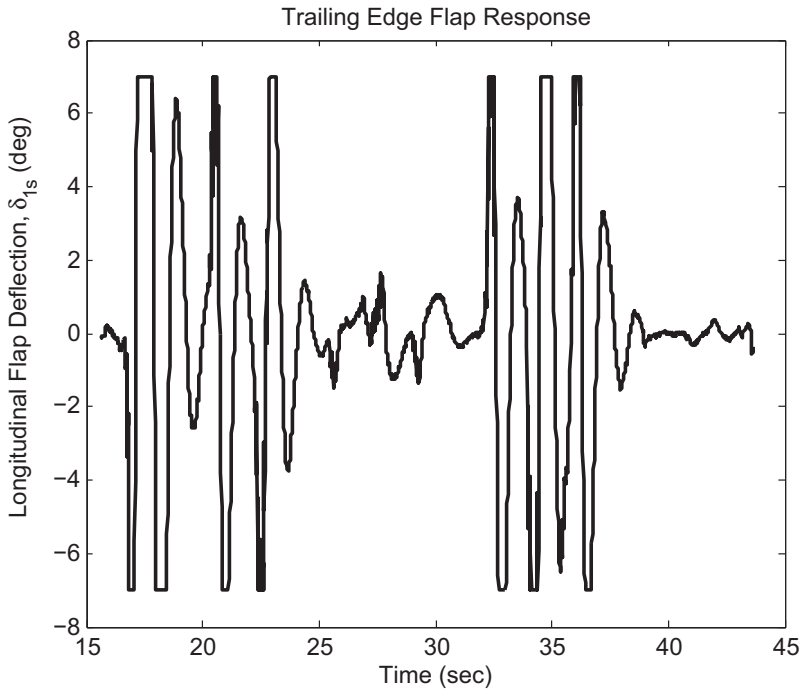

Figure 3.8. δ_{1s} flap response with ± 7 deg saturation and decreased pitch gain.

3.2 Actuator Rate Limit Response

The effect of rate limits on the swashplate actuators is examined by looking at natural frequency degradation of the actuator as well as variation of the frequency split threshold. The model is tested in the flight simulator with 25% rates of actuation on the swashplate.

3.2.1 Actuator Natural Frequency Degradation

Using the linear simulation, the natural frequency of the swashplate actuators was degraded to demonstrate the ability of the trailing edge flap controller to compensate for the limited bandwidth of the swashplate actuators. The results from the linear simulation are shown with the attitude response in Figure 3.9 and the angular rate response in Figure 3.10. The results show that as the response of the swashplate actuators begins to suffer from the reduced control rates, the attitude becomes less damped. As the natural frequency is decreased even further, the response of the vehicle will deteriorate to the point of becoming unstable.

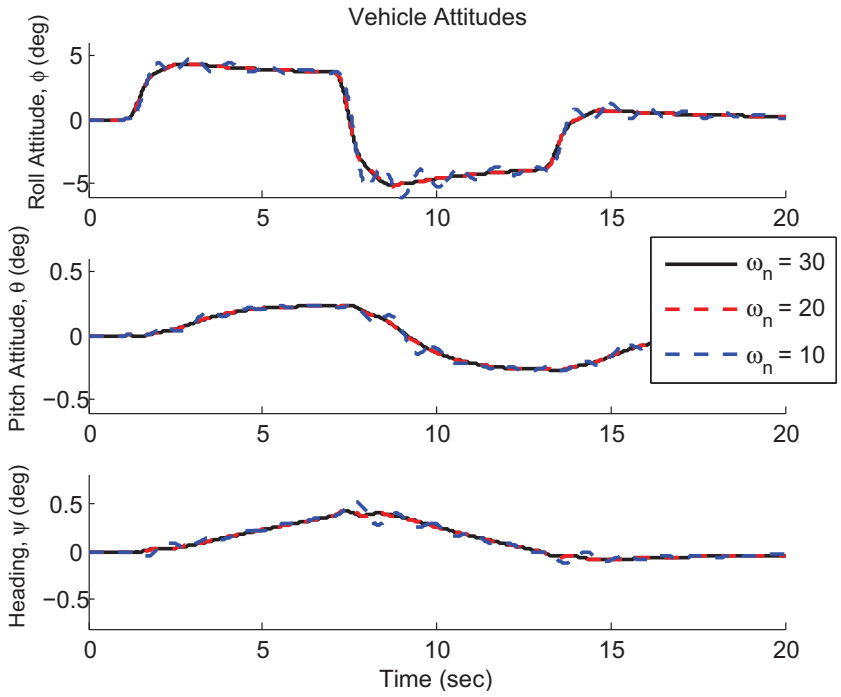

Figure 3.9. Attitude response to swashplate degradation without shared control.

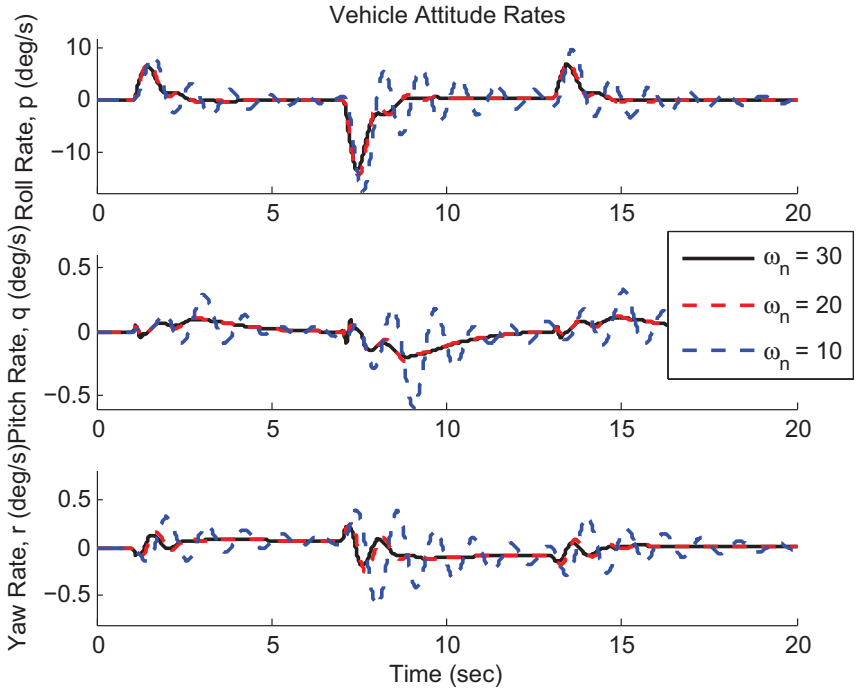

Figure 3.10. Rate response to swashplate degradation without shared control.

Using the trailing edge flaps in conjunction with the frequency splitting allocation can make up for some of the deficiency in the swashplate actuators. Figure 3.11 shows the result from the linear simulation of the same swashplate degradation, but with the trailing edge flaps taking over the high frequency commands. In this case, the command is 4.5 degrees in the lateral input which does not saturate the trailing edge flap actuators. As the natural frequency of the swashplate is degraded, the attitude remains close to the original because of the shared control. Although the result from the linear simulation is promising, the flight simulations do not show a significant improvement in control with degraded swashplate actuation.

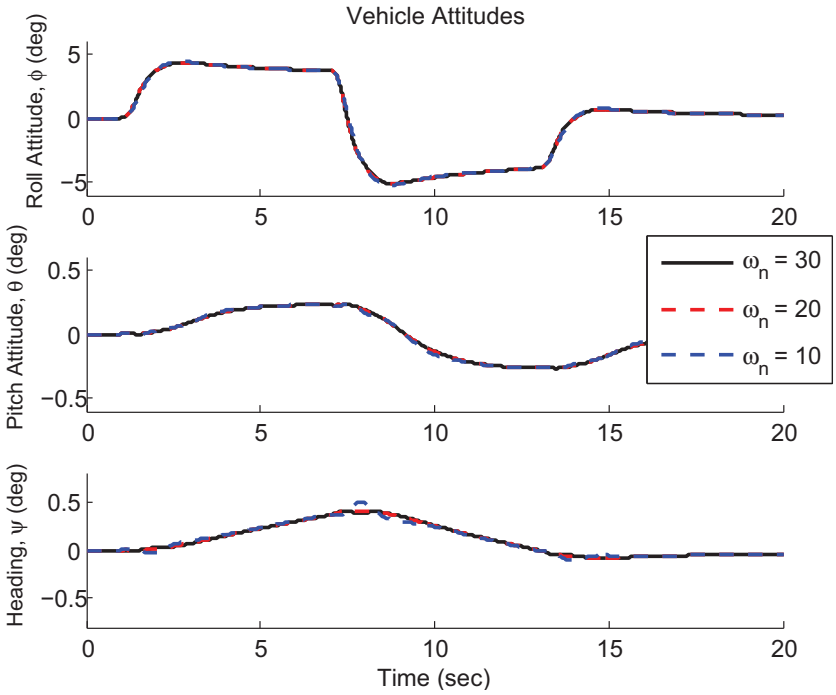

Figure 3.11. Attitude response to swashplate degradation with shared control.

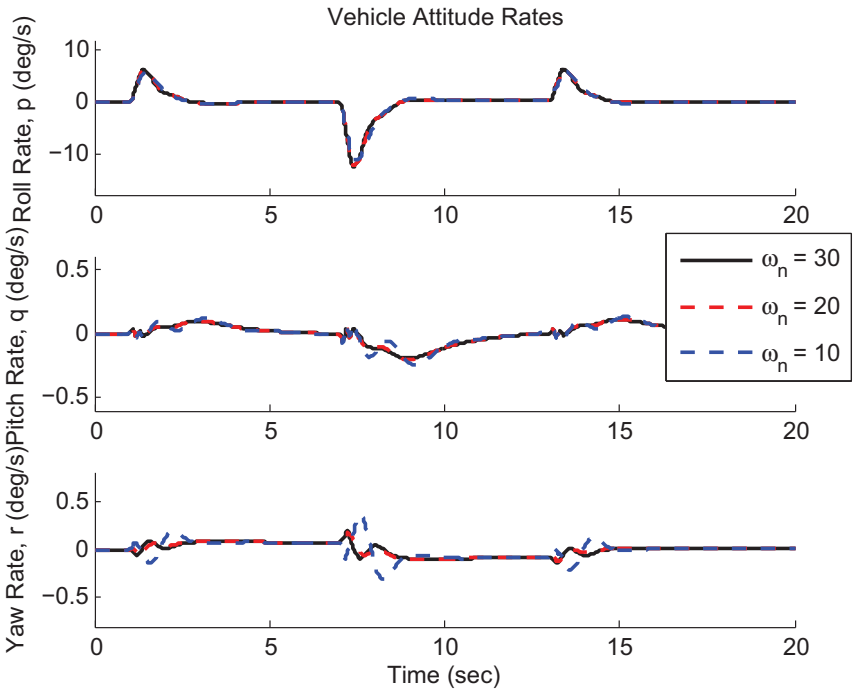

Figure 3.12. Rate response to swashplate degradation with shared control.

3.2.2 Rate Limiting

Section 2.4.1 detailed the theoretical rate limit imposed by the frequency based allocation of the control signals. The low pass filter on the swashplate signal caps the frequency at which the swashplate needs to respond to signals to ensure stable flight. For the flight simulation test, the swashplate actuators are degraded to 25% of their full rate capability. A flight simulation run was completed where a doublet was performed in the longitudinal direction with shared control enabled followed by another doublet with only the degraded swashplate actuator for primary control. Figure 3.13 shows the result of the test with the commanded pilot stick input. The second doublet, with only degraded control, does show a slower response with a smoothed response curve; however, in terms of flight handling, there was little discernable difference in handling from the pilot viewpoint.

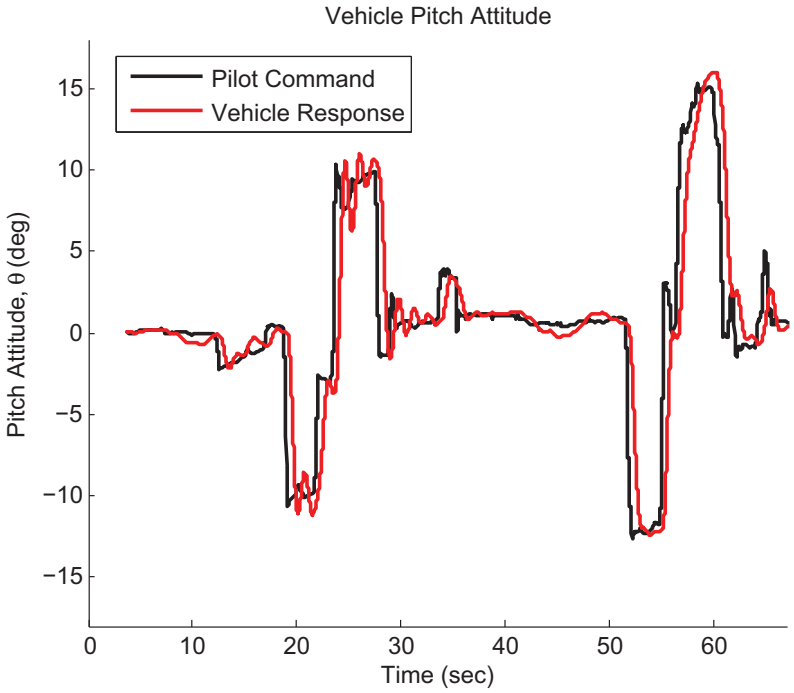

Figure 3.13. Pitch attitude response with degraded swashplate actuators.

3.3 Conclusion

After analyzing the results from both the linear simulations and the full piloted flight simulation, the results show that the range of response of the trailing edge flaps at a high frequency is limited in scope. The flaps do compensate for some of the control of the aircraft in degraded conditions; however, the actuators reach their travel limits before significant benefit is realized.

Though the control method was very limited with the current system and actuator models, further developments in the trailing edge flap models could eventually increase the benefit of control sharing with greater control authority and travel in the flaps. Implementation is primarily limited by the piezoelectric technology that is used to drive the actuators. Additionally, further modifications could be made to take into account the saturation limits and dynamically shift the frequency at which the allocation is split. While this would not define a strict rate limit on the system, it could result in better response with degraded systems than with the current fixed allocation scheme.

Appendix A

Simulation Data

A.1 Aircraft Parameters

Table A.1. UH-60A Rotor Properties

Parameter	Symbol	Value	Units
Number of Blades	N_b	4	
Radius	R	26.8	ft
Angular Velocity	Ω	258	RPM
Chord	c	1.73	ft
Shaft Tilt	Ω_{sx}	3	degrees forward
Lock Number	γ	6.5344	
Profile Drag Coefficient	C_{d0}	0.0076	
Blade Mass	M_b	7.79	slugs
Flap Hinge Offset	e_β	1.25	ft
Lag Hinge Offset	e_ζ	1.25	ft
1^{st} Flap Frequency	ν_β	1.04	
1^{st} Lag Frequency	ν_ζ	2.71	
1^{st} Torsion Frequency	ν_θ	4.27	
TEF Chord	c_f	20%	blade chord
TEF Span	b_f	75-95%	blade span

A.2 GENHEL Settings

Table A.2. Simulation Initial Conditions

Inital Conditions	Value	Units
Vehicle Weight	16825	lbs
Altitude	100	ft
Speed	0	knots
Pitch Attitude	0	deg
Roll Attitude	0	deg
Heading	0	deg
x CG offset	0	ft
y CG offset	0	ft

Table A.3. Control Settings Used in GENHEL Simulations

Active Controllers	Engine Control Unit
	Frequency Split Model Following Controller
Commands	Piloted Doublet Maneuvers
Time step	0.01 seconds
Wind	30 knot/30 deg WOD Conditions

Bibliography

[1] Wilkinson, C.H., Roscoe, M.F., and VanderVliet, G.M., "Determining Fidelity Standards for the Shipboard Launch and Recovery Task," *Proceedings of the AIAA Modeling and Simulation Technologies Conference and Exhibit*, Montreal, Canada, August 2001.

[2] Anon., "ADS-33D-PRF, Aeronautical Design Standard, Handling Qualities Requirements for Military Rotorcraft," United States Army Aviation and Troop Command, St. Louis, MO, May 1996.

[3] Johnson, W., *Helicopter Theory*, Dover Publications, Inc., New York, 1994.

[4] Padfield G.D., *Helicopter flight dynamics: The Theory and Application of Flying Qualities and Simulation Modelling*, AIAA Education Series, Blacksburg, 2007.

[5] Domke, B., "UH-60A Blackhawk" [Photograph], June 2001, Retreived March 20, 2010, from: http://www.bdomke.de/AviationImages/Rotorhead.html.

[6] Lau, B. H., Straub, F., Anand, V. R., and Birchette, T., "SMART Rotor Development and Wind-Tunnel Test," *Proceedings of the 35th European Rotorcraft Forum*, Hamburg, Germany, September 2009.

[7] Lee, D., "Simulation and Control of a Helicopter Operating in a Ship Airwake," Ph.D. Thesis, Department of Aerospace Engineering, The Pennsylvania State University, University Park, PA, August 2005.

[8] Horn, J.F., Bridges, D.O., and Lee, D., "Flight Control Design for Alleviation of Pilot Workload during Helicopter Shipboard Operations," *Proceedings of the American Helicopter Society 62nd Annual Forum*, Phoenix, AZ, May 9 -11, 2006.

[9] Horn, J.F., and Bridges, D.O., "A Model Following Controller Optimized for Gust Rejection during Shipboard Operations," *Proceedings of the American Helicopter Society 63rd Annual Forum*, Virginia Beach, VA, May 1 - 3, 2007.

[10] Shen, J. and Chopra, I., "Aeroelastic Modeling of Trailing-Edge-Flap Helicopter Rotors Including Actuator Dynamics," *Journal of Aircraft*, Vol. 41, No. 6, November-December 2004, pp. 1465-1481.

[11] Milgram, J. and Chopra, I., "A Parametric Design Study for Actively Controlled Trailing Edge Flaps," *Journal of the American Helicopter Society*, Vol. 43, No. 2, April 1998, pp. 110-119.

[12] Celi R., "Stabilization of Helicopter Blades with Severed Pitch Links Using Trailing-Edge Flaps," *Journal of Guidance, Control, and Dyanmics*, Vol. 26, No. 4, July-August 2003, pp. 585-592.

[13] Shen, J., "Comprehensive Aeroelastic Analysis of Helicopter Robot with Trailing-Edge Flap for Primary Control and Vibration Control," Ph.D. Thesis, Department of Aerospace Engineering, University of Maryland, College Park, MD, 2003.

[14] Shen, J. and Chopra, I., "Swashplateless Helicopter Rotor with Trailing-Edge Flaps," *Journal of Aircraft*, Vol. 41, pp. 208214, April 2004.

[15] Malpica, C. and Celi, R., "Simulation Based Bandwidth Analysis of a Swashplateless Rotor Helicopter," *Proceedings of the 63rd Annual Forum of the American Helicopter Society*, Virginia Beach, VA, May 2007.

[16] Duling, C.T., "Investigations on Primary Helicopter Control Using Trailing Edge Flaps," M.S. Thesis, Department of Aerospace Engineering, The Pennsylvania State University, University Park, PA, May 2009.

[17] Montanye, P., "Shipboard Helicopter Gust Response Alleviation Using Trailing Edge Flaps," M.S. Thesis, Department of Aerospace Engineering, The Pennsylvania State University, University Park, PA, August 2008.

[18] Howlett, J., "UH-60A BLACK HAWK Engineering Simulation Program: Volume I Mathematical Model," NASA CR-177542, USAAVSCOM TR 89-A-001, September 1989.

[19] Lee, D., Sezer-Uzol, N., Horn, J.F., and Long, L.N., "Simulation of Pilot Control Activity During Helicopter Shipboard Operations," *AIAA Journal of Aircraft*, Vol. 42, (2), March-April 2005, pp.448-461.

ACADEMIC VITA of Andrew D. Wilson

Andrew D. Wilson
4069 Tall Timber Drive
Allison Park, PA 15101
adwilson10@gmail.com

EDUCATION:

Bachelor of Science in Mechanical Engineering
The Pennsylvania State University
Schreyer Honors College, Spring 2010
Minors in Mathematics and Engineering Entrepreneurship
Honors in Aerospace Engineering
Thesis Title: A Control Allocation Method for a Helicopter with On-Blade Control
Thesis Supervisor: Dr. Joseph Horn

RELATED EXPERIENCE:

Internship with the NASA Robotics Academy
NASA Goddard Space Flight Center, Greenbelt, MD
Supervisor: Mr. John Vranish
Summer 2007

RISE Program (Research Internships in Science and Engineering)
Technische Universität München, Germany
Supervisor: Mr. Marwan Radi
Summer 2008

Internship with NASA Ames Research Center
Flight Vehicle Research & Technology Division
Moffett Field, CA
Supervisor: Dr. Carlos Malpica
Summer 2009

AWARDS:

NASA Aeronautics Scholarship Recipient
Harding Louis Memorial Scholarship Recipient
President's Freshman Award
PPG Industries Merit Scholarship
Dean's List

ACTIVITIES:

Penn State Marching Blue Band
Penn State Robotics Club
Penn State NanoSat Program